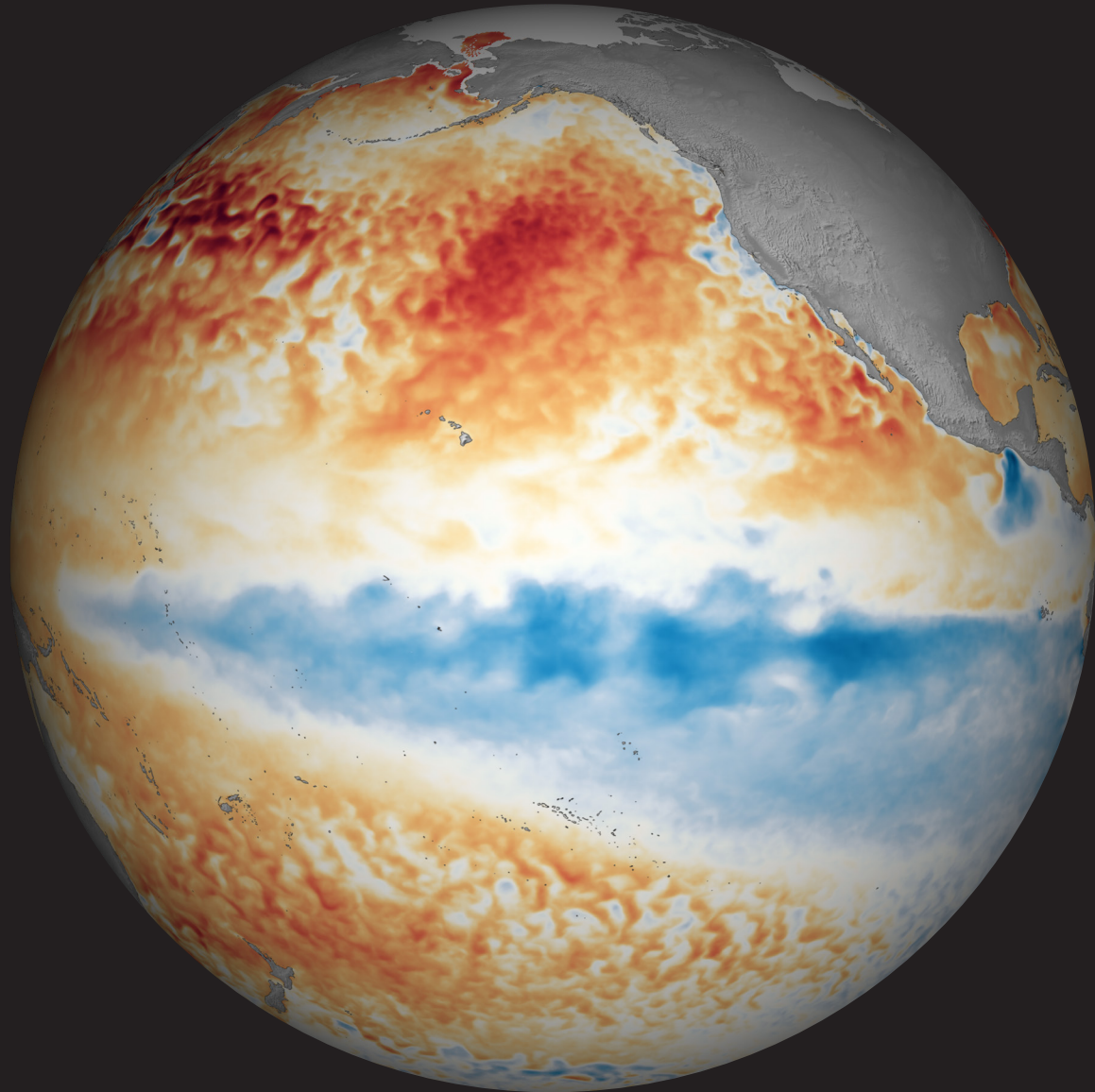


# STATE OF THE CLIMATE IN 2020

## THE TROPICS

H. J. Diamond and C. J. Schreck, Eds.



Special Online Supplement to the *Bulletin of the American Meteorological Society* Vol.102, No. 8, August, 2021

<https://doi.org/10.1175/BAMS-D-21-0080.1>

Corresponding author: Howard J. Diamond / [howard.diamond@noaa.gov](mailto:howard.diamond@noaa.gov)

©2021 American Meteorological Society

For information regarding reuse of this content and general copyright information, consult the [AMS Copyright Policy](#).

# STATE OF THE CLIMATE IN 2020

## THE TROPICS

### Editors

Jessica Blunden  
Tim Boyer

### Chapter Editors

Freya Aldred  
Peter Bissolli  
Howard J. Diamond  
Matthew L. Druckenmiller  
Robert J. H. Dunn  
Catherine Ganter  
Nadine Gobron  
Gregory C. Johnson  
Tim Li  
Rick Lumpkin  
Ademe Mekonnen  
John B. Miller  
Twila A. Moon  
Ahira Sánchez-Lugo  
Ted A. Scambos  
Carl J. Schreck III  
Sharon Stammerjohn  
Richard L. Thoman  
Kate M. Willett

### Technical Editor

Andrea Andersen

### *BAMS* Special Editor for Climate

Michael A. Alexander

American Meteorological Society

system developed, Subtropical Storm Alpha developed in the eastern North Atlantic basin. The upper air aspects of the two systems were similar with cold core cut-off low precursors analyzed at the 700-hPa and 500-hPa levels, a feature that has been previously associated with tropical transition (TT; Pantillon et al. 2013).

The second system (Fig. SB4.4) developed on 20 November from an extratropical system between Italy and Sardinia, and underwent TT prior to crossing the western tip of Sicily (TT of baroclinic systems has been documented as a contributing factor to the development of medicanes [Mazza et al. 2017]). An eye-like feature then developed on 22 November prior to

landfall in Tunisia. Maximum winds were estimated to have reached 40 kt ( $20 \text{ m s}^{-1}$ ) during the tropical phase.

The last system (Fig. SB4.4) developed south of Turkey on 14 December following the TT of a precursor system, then traveled east along the southern Cypriot coastline. A second landfall occurred along the Syrian coast while the remnant cloud mass tracked to near the Syria-Iraq border. Maximum winds were estimated around 45 kt ( $23 \text{ m s}^{-1}$ ). So, while the medicanes is an area still open for debate in the tropical cyclone community, it is still an interesting feature, and to have three fairly significant such storms during the 2020 season was a topic considered as sufficiently interesting to highlight in this year's report.

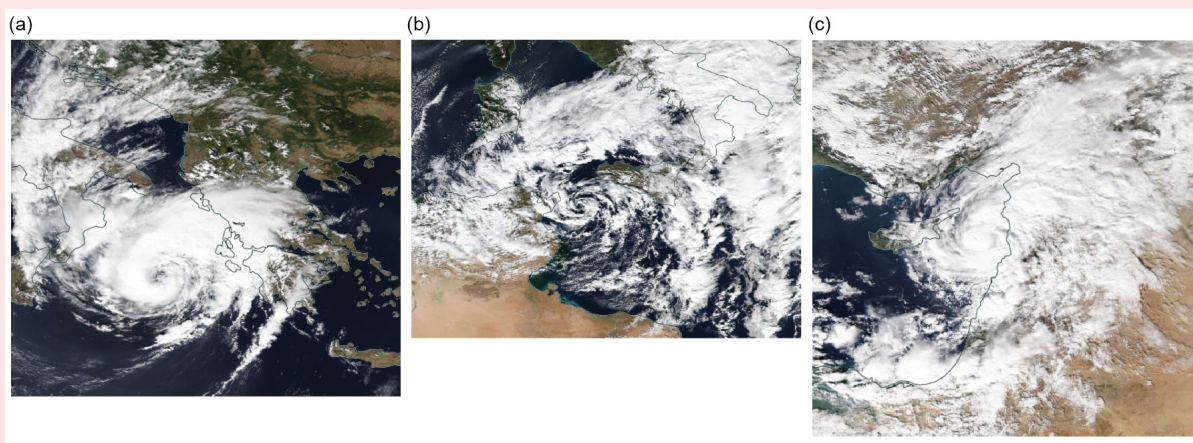


Fig. SB4.4. System #1, 17 Sep (NOAA 20); System #2, 21 Nov (Aqua); and System #3, 16 Dec (Aqua). Imagery courtesy of NASA Worldview.

#### h. Tropical cyclone heat potential—R. Domingues, G. J. Goni, J. A. Knaff, I-I Lin, and F. Bringas

In this section, upper-ocean heat content conditions based on the tropical cyclone heat potential (TCHP; e.g., Goni et al. 2009; 2017) are described as anomalies with respect to the long-term mean (1993–2019) and differences to conditions observed in 2019. TCHP quantifies the excess heat content between the sea surface and the depth of the 26°C isotherm (D26, the minimum temperature required for genesis and intensification; Leipper and Volgenau 1972; Dare and McBride 2011) and provides information about the amount of heat stored in the upper ocean and available to fuel TC intensification. As in this section, TCHP is often used as a convenient guide of pre-TC ocean thermal conditions because it carries information about the integrated upper-ocean thermal profile (from sea surface temperature [SST] to D26). High TCHP before a TC usually leads to a smaller amount of SST cooling during a TC, and hence higher enthalpy fluxes from the ocean into the storm, favoring intensification (e.g., Lin et al. 2013). Similarly, upper-ocean salinity is another condition of relevance for TC intensification because freshwater-induced barrier layers may also modulate the upper ocean mixing and cooling during a TC, and hence the air–sea fluxes (e.g., Balaguru 2012; Domingues et al. 2015). Areas in the ocean with pre-TC TCHP values above  $50 \text{ kJ cm}^{-2}$  have been associated with TC intensification (e.g., Shay et al. 2000; Mainelli et al. 2008; Lin et al. 2014, Knaff et al. 2018), provided that atmospheric conditions are also favorable.

TCHP seasonal anomalies (Fig. 4.41) are calculated as departures from the long-term mean (1993–2019) for the primary months of TC activity in each hemisphere: June–November 2020 in the Northern Hemisphere (NH) and November 2019–April 2020 in the Southern Hemisphere (SH). Differences between the 2020 and 2019 seasons are also analyzed (Fig. 4.42). In any of the regions highlighted in Fig. 4.41 in which TCs are known to form and intensify, TCHP anomalies generally exhibit large spatial and temporal variability due to mesoscale features and short- to long-term modes of variability (e.g., El Niño–Southern Oscillation [ENSO]) and trends.

The 2020 TC season exhibited above the mean 1993–2019 TCHP values in most of the tropical cyclone basins (Fig. 4.41), suggesting that conditions for TC development and intensification were generally favorable in terms of upper-ocean heat content. Notable anomalies with values as large as  $30 \text{ kJ cm}^{-2}$  above the long-term mean were observed in the North Indian, South Indian, and West Pacific basins, and in the western Caribbean Sea and parts of the Gulf of Mexico. Compared to 2019, TCHP values also increased in all basins (Fig. 4.42), with the exception of the East Pacific, where lower TCHP values observed in 2020 were associated with an ongoing La Niña event (additional details below).

In the SH, TCHP was anomalously elevated in the southwest Indian Ocean (IO) and beyond the date line during the TC season, and was near normal elsewhere (Fig. 4.41). The observed TC activity was slightly elevated in the southwest IO, which included TC Herold that skirted north of Mauritius. Harold formed near the Solomon Islands and later rapidly intensified before making landfall on Espiritu Santo and Pentecost Islands, Vanuatu, at Category 5 intensity. See section 4g8 for details of this storm.

In the IO, as indicated earlier, all three TC basins exhibited above-normal TCHP conditions (Fig. 4.41), with anomalies up to  $\sim 30 \text{ kJ cm}^{-2}$  above the long-term average in the North IO basin inside the Bay of Bengal and in the southwest IO basin. All three basins also exhibited notable warming of  $20 \text{ kJ cm}^{-2}$  compared to values observed in 2019 (Fig. 4.42). In fact, the 2020 TCHP values were generally within the  $80\text{--}100 \text{ kJ cm}^{-2}$  range in the Bay of Bengal and southwest IO basin. Associated with these upper-ocean conditions, the North IO basin exhibited above-average TC activity, the southwest IO basin exhibited slightly above-normal

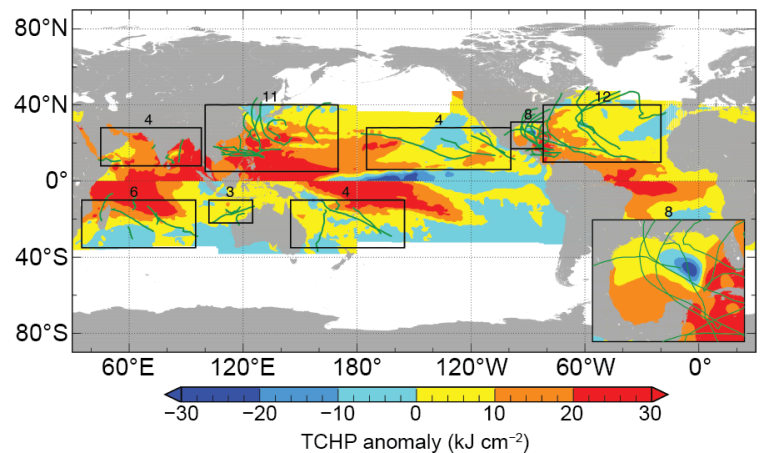


**Fig. 4.41.** Global anomalies of TCHP during 2020 computed as described in the text. The boxes indicate the seven regions where TCs occur: from left to right, southwest Indian, North Indian, west North Pacific, southeast Indian, southwest Pacific, east Pacific, and North Atlantic (shown as Gulf of Mexico and tropical Atlantic separately). The green lines indicate the trajectories of all tropical cyclones reaching at least Category 1 strength ( $\geq 64 \text{ kt}$ ,  $34 \text{ m s}^{-1}$ ) and above during Jun–Nov 2020 in the NH and Nov 2019–Apr 2020 in the SH. The numbers above each box correspond to the number of Category 1 and above cyclones that traveled within each box. The Gulf of Mexico conditions are shown in the inset in the lower right corner.

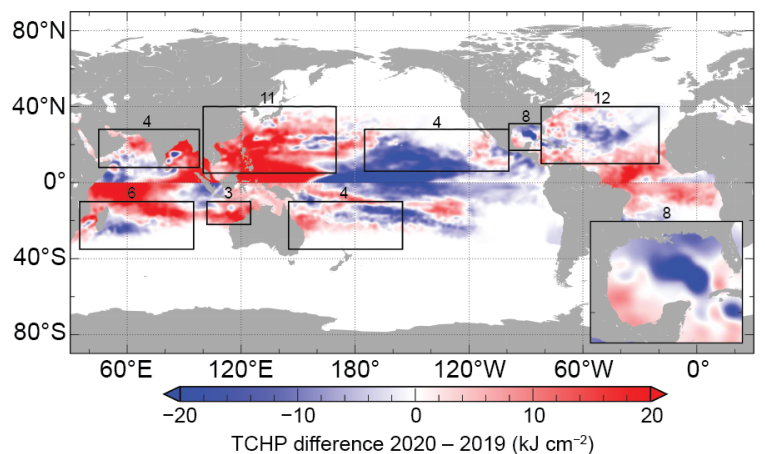


**Fig. 4.42.** TCHP anomaly difference ( $\text{kJ cm}^{-2}$ ) between the 2020 and 2019 tropical cyclone seasons (Jun–Nov in the NH and Nov 2019–Apr 2020 in the SH).

TC activity, and the southeast IO basin exhibited normal activity. With the above-average activity observed in the North IO basin, the 2020 TC season was also the costliest on record, largely due to Cyclone Amphan (16–21 May), which underwent rapid intensification over the anomalously large TCHP in the Bay of Bengal. Similarly, TC Gati, which was the most intense (100 kt,  $51 \text{ m s}^{-1}$ ) to make landfall in Somalia since at least the start of the satellite era, rapidly and unexpectedly intensified over warm TCHP anomalies before striking land.

In the North Pacific, the ENSO state generally plays a large role in defining the large-scale upper-ocean thermal conditions that can impact both the eastern and western North Pacific basins (e.g., Lin et al. 2014, 2020; Zheng et al. 2015). In early 2020, ENSO transitioned from a weak positive phase to a negative phase by mid-year. La Niña conditions developed in August and persisted throughout the entire 2020 TC season. Associated with this ENSO state, TCHP values increased by over  $20 \text{ kJ cm}^{-2}$  in the western North Pacific and decreased by  $20 \text{ kJ cm}^{-2}$  in the eastern North Pacific basins with respect to conditions seen in 2019 (Fig. 4.42). Despite these changes, TCHP values were still  $10\text{--}20 \text{ kJ cm}^{-2}$  and  $30 \text{ kJ cm}^{-2}$  above the long-term mean in the eastern North Pacific and western North Pacific basins, respectively.

While upper-ocean conditions were warmer than normal, which is generally conducive for TC genesis and intensification, TC frequency in the western North Pacific basin was below average in 2020, as often found in La Niña years (Lin et al. 2020). This is because TC frequency in this basin is primarily controlled by atmospheric dynamics (Lin and Chan 2015) rather than by upper-ocean conditions. Despite the overall lower TC activity, large TCHP values likely contributed to the significant intensification of several storms in this basin, as also observed in previous La Niña or La Niña-like years (e.g., TC Megi in 2010, TC Haiyan in 2013; Lin et al. 2014). Among those, Super Typhoon Goni was a notable example. Goni developed south of Guam and followed a similar track to TC Haiyan in 2013 in the southwestern North Pacific main development region (Lin et al. 2014; i.e., east of the Philippines between  $5^{\circ}\text{N}$  and  $20^{\circ}\text{N}$ ). As it traveled over areas characterized by high SSTs and high TCHP values (not shown), it experienced a very rapid intensification of  $80 \text{ kt}$  ( $41 \text{ m s}^{-1}$ ) during a 24-hour window, surpassing Haiyan's  $60\text{-kt}$  intensification. Goni eventually reached the same record intensity of  $170 \text{ kt}$  ( $87 \text{ m s}^{-1}$ ) as Haiyan in 2013 before making landfall in the Philippines.

In the eastern North Pacific basin, there was an average number of TCs but a below-average number of hurricanes. The La Niña conditions observed in the North Pacific, which were associated with negative SST anomalies (not shown) and lower TCHP values compared to 2019 (Fig. 4.42), likely contributed to the reduced hurricane activity in this basin during the 2020 season.

The North Atlantic basin exhibited TCHP values  $10\text{--}20 \text{ kJ cm}^{-2}$  above the long-term mean in most areas within this basin (Fig. 4.41). Compared with conditions recorded in 2019, TCHP values were also approximately  $10 \text{ kJ cm}^{-2}$  larger in value for 2020 within the western Caribbean Sea, southern Gulf of Mexico, and along the southeast U.S. coast. A notable increase in TCHP values was observed in the western Caribbean Sea, where TCHP was approximately  $30 \text{ kJ cm}^{-2}$  larger-than-average conditions, with absolute values typically above  $100 \text{ kJ cm}^{-2}$  and as large as  $140 \text{ kJ cm}^{-2}$  (not shown). Associated with these conditions, the North Atlantic basin recorded unprecedented levels of TC activity (section 4g2). From the 14 TCs that reached Category 1 intensity, eight traveled through the open North Atlantic, Caribbean Sea, and Gulf of Mexico (Fig. 4.41). Hurricane Hanna (23–27 July) was the only system to develop and intensify strictly within the Gulf of Mexico. The positive TCHP anomalies observed in 2020 provided the favorable ocean conditions that likely contributed to this very intense TC activity, especially in the western Caribbean Sea, where Category 4 Hurricanes Delta (5–12 October), Eta (31 October–14 November), and Category 4 Hurricane Iota (13–18 November) reached their peak intensity. Iota, for example, rapidly intensified into a Category 5 hurricane over extremely anomalously high TCHP values for November.

In summary, the 2020 TC season exhibited positive TCHP anomalies in most of the TC basins (Fig. 4.41), with notable increases in the upper-ocean heat content in the North Indian, South Indian, and western North Pacific basins, and the western Caribbean and southern Gulf of Mexico. While this could suggest that upper-ocean conditions conducive for TC development and intensification were anomalously favorable in these basins in terms of upper-ocean heat content, in fact, global TC activity in terms of ACE was below normal in association with the La Niña conditions in place. In fact, some of the notable TCs of 2020 highlighted above, such as Cyclone Amphan in the North Indian Ocean, Super Typhoon Goni in the West Pacific, and Hurricane Iota in the Atlantic, underwent rapid intensification while traveling over areas with large TCHP values. In the Pacific Ocean, upper-ocean thermal conditions and TC activity were largely modulated by an ongoing La Niña, which likely caused below-normal TC activity in both the eastern and western North Pacific basins. In the Atlantic, a record number of named TCs were observed, with several major hurricanes reaching their peak intensity while traveling over the anomalously warm western Caribbean Sea. The 2020 season also featured the development of three hurricane-like cyclones or “medicanes” that were recorded within the Mediterranean Sea and were associated with positive SST anomalies.